High-resolution sequence stratigraphic division and distribution of tidal deposits in the Zhuhai Formation, Huizhou Sag, Pearl River Mouth Basin, South China Sea

WENBO ZHENG* & HONGWEN DENG

School of Energy Resources, China University of Geosciences (Beijing), 29 Xueyuan Rd, Beijing 100083, China

Abstract – The Zhuhai Formation of the Huizhou Oilfield has been interpreted as being deposited in a tide-dominated estuarine setting. This paper uses stratigraphic principles, cores and logging data to analyse the facies changes of tidal sedimentation in response to the base level cycle. We conclude that the mud flat progradational allocycle is the result of a long-term base level fall, while the fining-upwards autocycle is in response to a short-term base level fall. Region-wide mud layers of supratidal zones and scour surfaces of subtidal zones are stratigraphic surfaces of tidal sedimentation. By integrating high-resolution stratigraphic correlations with seismic attributes extracted from the stratal slicing of 3-D data volumes, we use an attribute map of RMS (root mean square) amplitude to image the distribution and evolution of tidal deposits in the study area. Intertidal zones and the upper parts of the tidal cycle are favourable areas for prospecting and oil reserves and thus provide a basis for petroleum exploration and development.

Keywords: stratigraphy, stratal slicing, seismic attribute, tidal deposition, Zhuhai Formation, Huizhou Oilfield.

1. Introduction

The Huizhou Oilfield is a source of hydrocarbons from the Oligocene Zhuhai Formation of the Pearl River Mouth Basin, South China Sea. This oilfield is approximately 190 km southeast of Hong Kong and has an area of 160 km². The principal reservoir of the Oligocene Zhuhai Formation is tidal sandstone (Deng & Zheng, 2009). Previous studies show that the distribution, complexity and variability of the reservoir's properties are quite different from those of the other reservoirs in the eastern South China Sea (Chen *et al.* 1998; Li *et al.* 2007; Wei *et al.* 2008).

Sequence stratigraphic analysis has provided a major advance in the understanding of sediment partitioning between nonmarine, shallow and deep marine sedimentary environments in relatively simple tectonic settings, such as passive margins and foreland basins (Van Wagoner *et al.* 1990; Shanley & McCabe, 1991). It is possible to image depositional trends and to predict infill locations that will hold these reservoirs using seismic attributes extracted from 3-D data volumes (Horn *et al.* 2001). In this paper, a stratigraphic framework is established by the analysis of tidal sedimentation in response to a base level cycle, and we use a seismic attribute map extracted from stratal slicing to image the tidal sandstone reservoir in the Zhuhai Formation.

2. Geological settings

The Huizhou Oilfield is bounded by a step-fault zone to the north, resulting in tectonic activity, and the Dongsha Uplift to the south, which consists of basement volcanic rock (Carnes *et al.* 1994) (Fig. 1). The Oligocene Zhuhai and Miocene Zhujiang formations are separated by regional unconformity T6 (Fig. 2).

The sediment source of the Zhuhai Formation in the Huizhou Oilfield is the north Pearl River. The Dongsha Uplift is only a source for its nearby area. The Dongsha Uplift, which is high in the east and low in the west, was a barrier peninsula during the time of deposition of the Zhuhai Formation, and it flooded gradually by transgression during the deposition of the Zhujiang Formation (Fig. 3). This palaeogeography provides good conditions for tidal deposition. The central part of the Huizhou Sag is composed of subtidal deposits that gradually change to intertidal and supratidal deposits and that overlap the northern region and the southern Dongsha Uplift (Fig. 3).

3. Tidal sedimentary succession

Shanmugam, Poffenberger & Toro Alava (2000) described the typical structures of tidal sedimentation. Deng & Zheng (2009) documented seven typical sedimentary structures of tidal deposits in cores of the Zhuhai Formation, such as tidal bedding, structureless bedding, graded and rhythmic bedding, mud drapes and couplets, herringbone cross-bedding, reactivation surfaces, and parallel-cross-stratification (Fig. 4).

The energy of the tide gradually weakens from a subtidal to supratidal zone, and it leads to a seaward

* Author for correspondence: zhengwenbo520@yahoo.com.cn
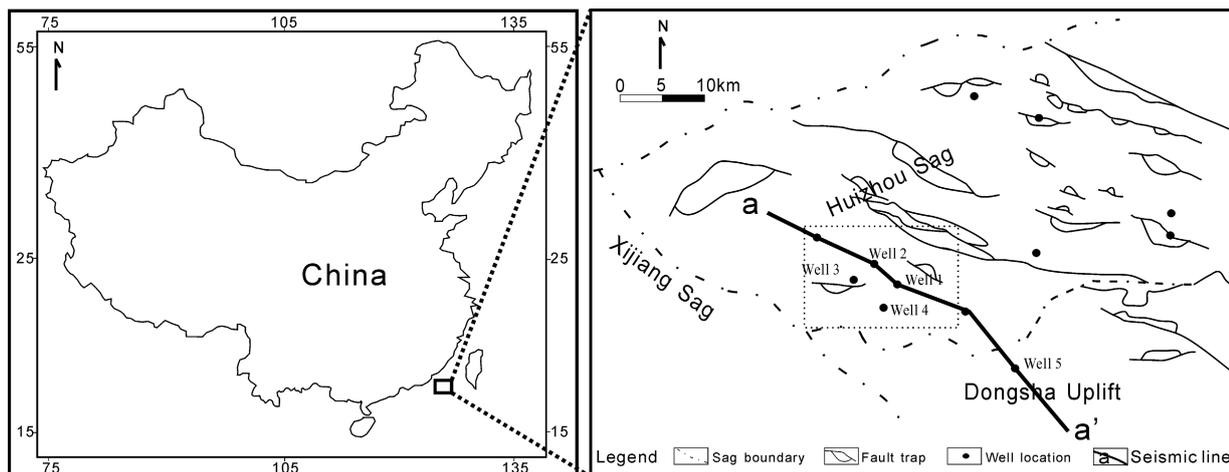
Figure 1. Scope of the study area in the South China Sea. The study area is bounded by the Dongsha Uplift in the south.

Figure 2. Stratigraphic column. The Zhuhai Formation is deposited in a tidal and coastal setting.

decrease in mud content and increasing grain size (Deng & Zheng, 2009). A typical tidal sedimentary sequence is an overall fining-upwards succession that consists of a combination of tidal channel, tidal bar, sand flat and mud flat deposits. The base of a tidal channel is marked by a scour and lag and will typically be followed by a fining-upwards succession of cross-bedded sands, which may show mud drapes, inclined heterolithic stratification and bi-directional palaeocurrent indicators. Muddy tidal flat deposits rich in organic material may contain sandy sediments deposited within tidal creeks at the highest tides (Fig. 5).

4. Analytical methods

4.a. Stratigraphy

Wheeler (1964) succinctly reviewed the use of the term 'base level' in stratigraphy, and Cross (1992) clearly demonstrated how the concept of base level has direct application to sequence stratigraphy. Base level, in a stratigraphic sense, is not a real, physical surface but rather an abstract surface that represents the equilibrium between erosion and deposition. The base level cycle determines the preservation of the sequence and differentiation within a single facies.
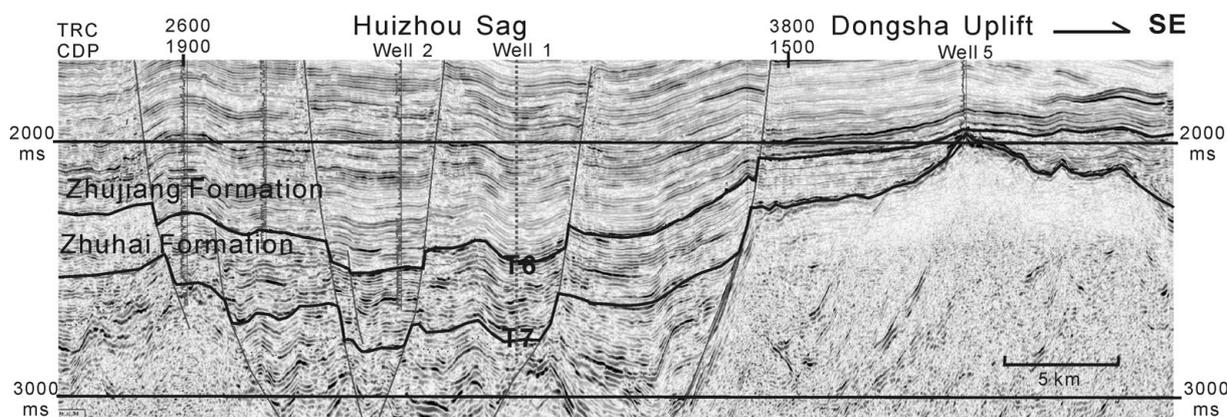
Figure 3. Seismic profile showing stratigraphic characteristics and distribution of the Zhuhai Formation in the Huizhou Sag (for location of section line a–a′ see Fig. 1).
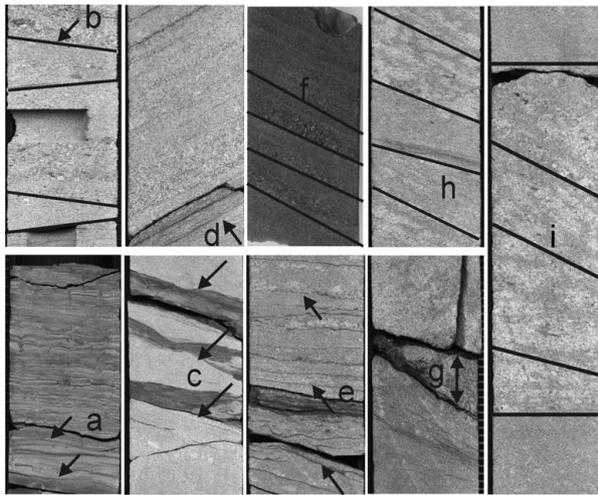
Figure 4. Tidal sedimentary structures in the Zhuhai Formation. (a) Tidal bedding (well 2, 3682.0 m). (b) Bidirectional cross-stratification (well 2, 3688.2 m). (c) Mud drapes in sandstone show units of rhythmic alternation (well 2, 3905.6 m). (d) Cross-bedded sandstone with double mud layers which represents a period of slack-water deposition (well 2, 3911.1 m). (e) Fine sandstone with double mud layers (well 2, 3915.9 m). (f) Rhythmic graded sandstone. Ebb tide with high velocity carries coarse sediments, while flood tide with low velocity carries fine particles (well 1, 3921.2 m). (g) Tangential contacts and mud-draped toeset (well 1, 3914.7 m). (h) Reactive surface (well 1, 3906.5 m). (i) Parallel and cross-stratifications in tidal bundle; high angle, thicker tidal sand bundle deposited in spring tide, while low angle, thinner sand bundle deposited in neap tide (well 1, 3915.2 m).

It should be noted that a change in particle size is a good indicator for facies, but fining upwards cannot be taken as an indicator of deepening water depth (Deng & Zheng, 2009). Generally, a base level rise suggests a reduction in hydrodynamic energy and the development of muddy sediments, but this is the opposite in tidal deposition. On a tidal coast, a base level fall means a relative shallowing of water depth and the deposition of mudstone in a low hydrodynamic energy environment, while a base level rise represents a relative deepening of the water depth and sandstone deposition in a high hydrodynamic energy environment. The base level peak forms coarse and thick herringbone cross-bedded sandstone, while the base level trough forms black coal or plant debris and burrowed mudstone (Fig. 6). Therefore, a prograding and fining-upwards tidal flat is the result of base level fall, while transgressive tidal channel formation and filling are the products of base level rise (Fig. 6).

In the tidal succession of a short-term base level cycle, which is called an autocycle, the thickness range is 20–25 m. In the tidal succession of a long-term base level cycle, which is called an allocycle, the thickness range is 100–120 m. The sandy deposits of a subtidal zone correspond to a high base level phase, while mud interbedded with the thin sand of an intertidal zone corresponds to a low base level phase (Fig. 7).

The progradation of tidal flats tends to produce a fining-upwards sequence, which reflects a transition from low tide level sand flats upwards into high tide level mudflats and eventually into supratidal flats. This sequence may be cut at any level, and in some cases be completely replaced, by erosive-based tidal channel sequences (Reineck, 1972; Mackenzie, 1972; Evans, 1975) (Fig. 7).

Region-wide mudflats that correspond to a lower base level or a scoured surface of an erosive-based tidal channel that corresponds to a high base level can be marker horizons and stratigraphic surfaces of tidal sedimentation. Guided by this correlation strategy, Cycle 5 of the Zhuhai Formation can be divided into precise sub-cycles. The boundaries are region-wide scour surfaces, such as sb5 of well 2–4 and sb6 of well 2. The sub-surfaces of Cycle 5, sb5-a and sb5-b, are
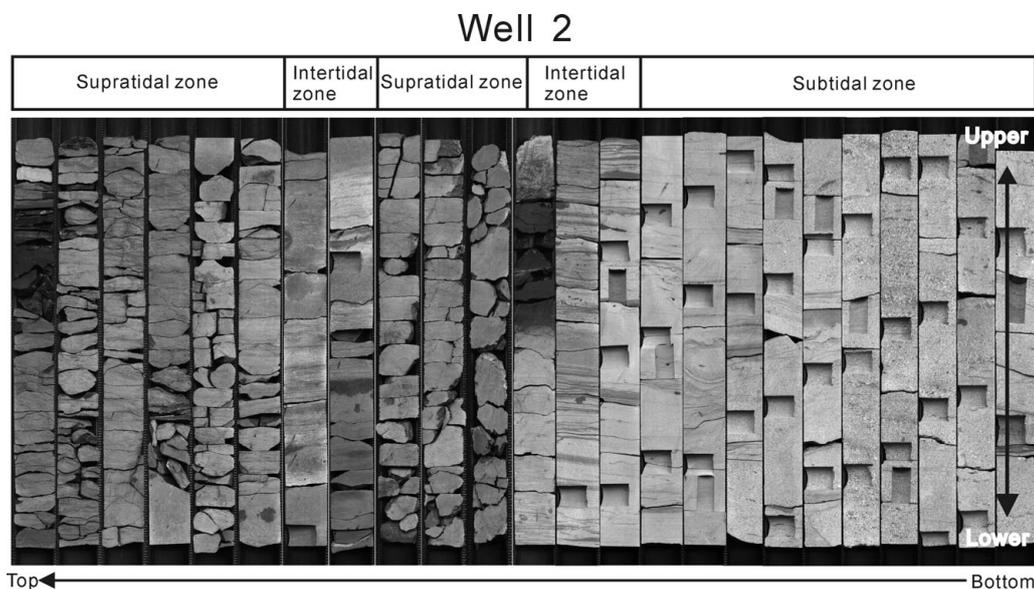
Well 2

Figure 5. Typical tidal sedimentary succession in core of well 2.
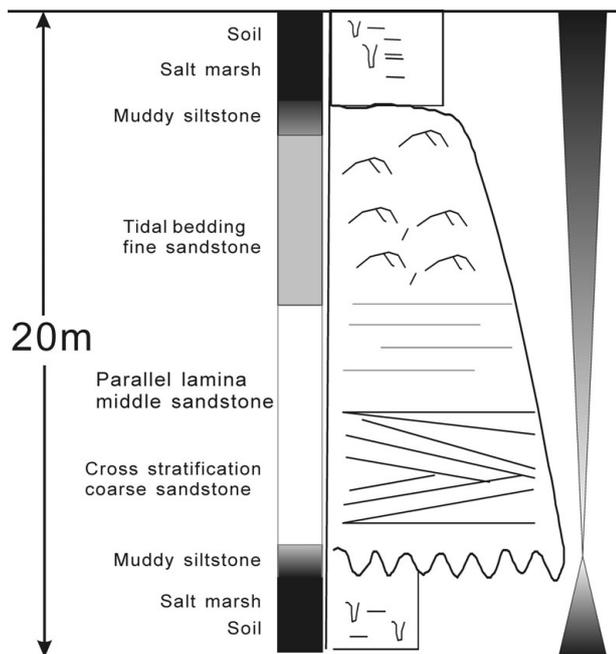
Figure 6. Autocycle of tidal succession in base level cycle.

oilfield-wide mud marker horizons or scour surfaces with minimum erosion (Fig. 8).

4.b. Stratal slicing

With the guidance of a modern depositional model, using seismic attributes and logging data to analyse sedimentary facies has become an effective geophysical tool for reservoir prediction in recent years.

There are three slicing methods, including time slicing (Fig. 9a), surface slicing (Fig. 9b) and stratal slicing (Fig. 9c). Zeng *et al*. (1998) concluded that 'stratal slicing is a useful new tool for basin analysis and reservoir delineation by making depositional facies mapping an easier task, especially in wedged depositional sequences. Stratal slicing on a workstation is done by first tracking frequency-independent, geologic-time-equivalent reference seismic events, then building a strata-time model and an amplitude stratal slice volume on the basis of linear interpolation functions between references.'

Although the bases and tops of a tidal sequence can be mapped over the study interval, well logs show that the distribution of sand and mud is complex and impossible to correlate or define deterministically. In consideration of the wedge-shaped strata of Cycle 5, we use the stratal slicing method here. After well-to-seismic tie, we track the seismic surfaces sb5 and sb6 to establish the stratigraphic framework. Being restricted by the resolution of the seismic data, the appropriate slicing of Cycle 5 is into three equal subintervals of thicknesses of 30–40 m and times of 13–15 ms.

4.c. Seismic attribute mapping

Attributes extracted from the time window of stratal slicing are more reliable for the identification of high-resolution stratigraphic cycles in the sedimentary system. Because amplitudes are squared before averaging, the root mean square (RMS) computation is highly sensitive to extreme amplitude values of lithological
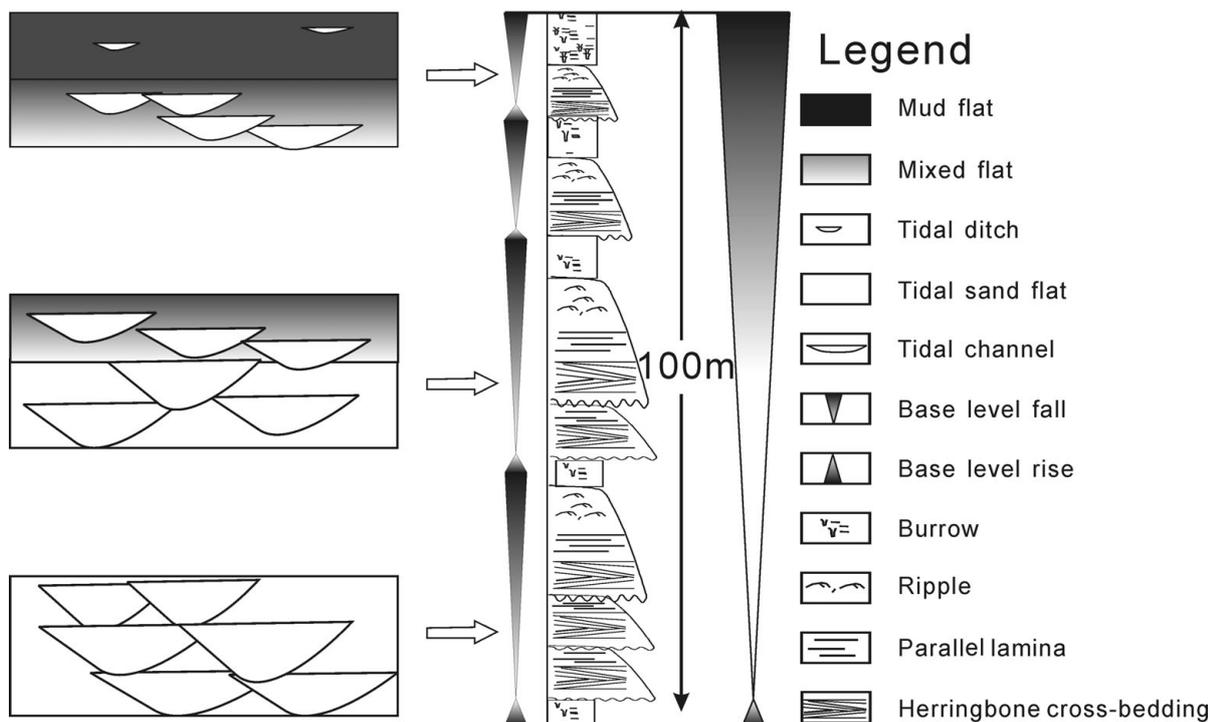
Figure 7. Relative preservation of tidal facies in a long-term base level cycle.
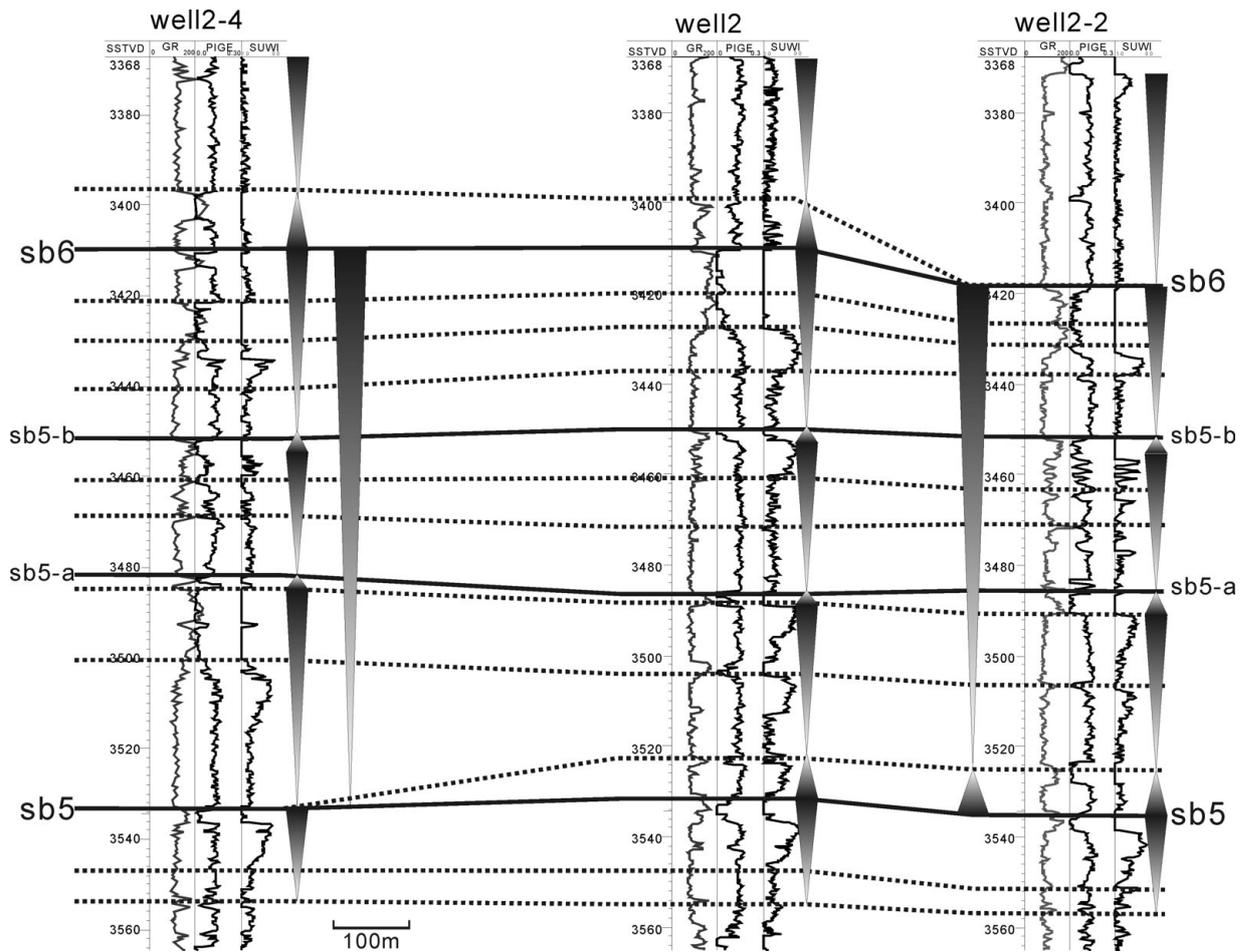
Figure 8. Stratigraphic division and correlation of Cycle 5.

boundaries (Bruce, 2002; Chopra & Marfurt, 2008). By integrating high-resolution stratigraphic correlations with seismic attributes extracted from 3-D data volumes, it is possible to image the depositional trends of tidal sandstones that will encompass these reservoirs.

5. Results

Attribute maps of RMS amplitude were extracted from the stratal slicing of Cycle 5 (Fig. 10a, b, c). It is advisable that the seismic observations be calibrated
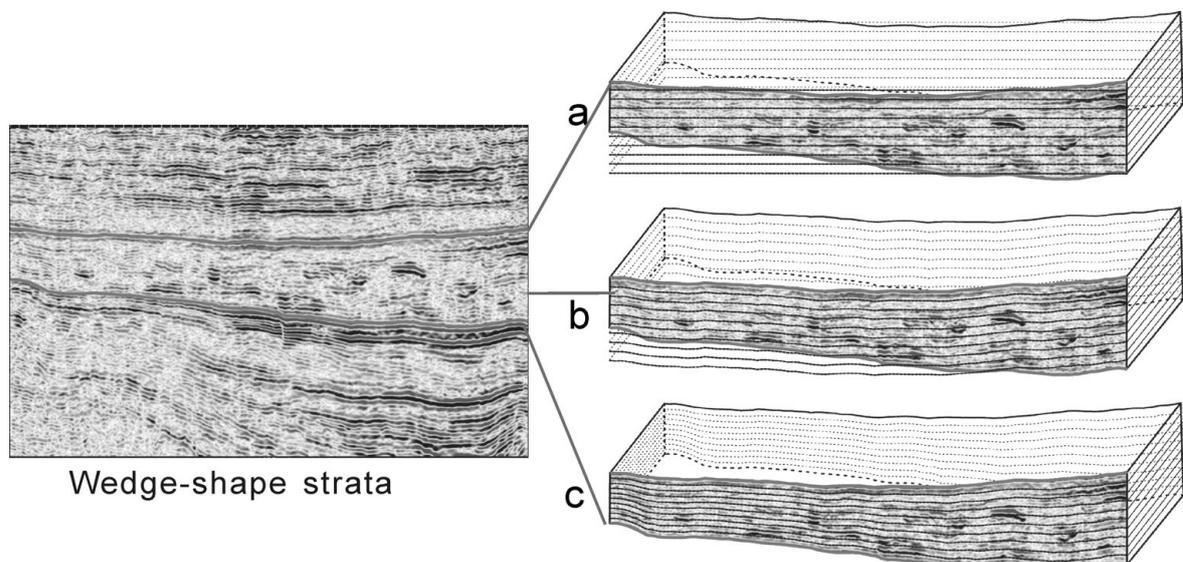
Figure 9. Comparison of different slicing methods in wedge-shaped strata. (a) Time slicing; (b) horizon slicing; (c) stratal slicing. Time and horizon slicing are diachronous in wedge-shaped strata.
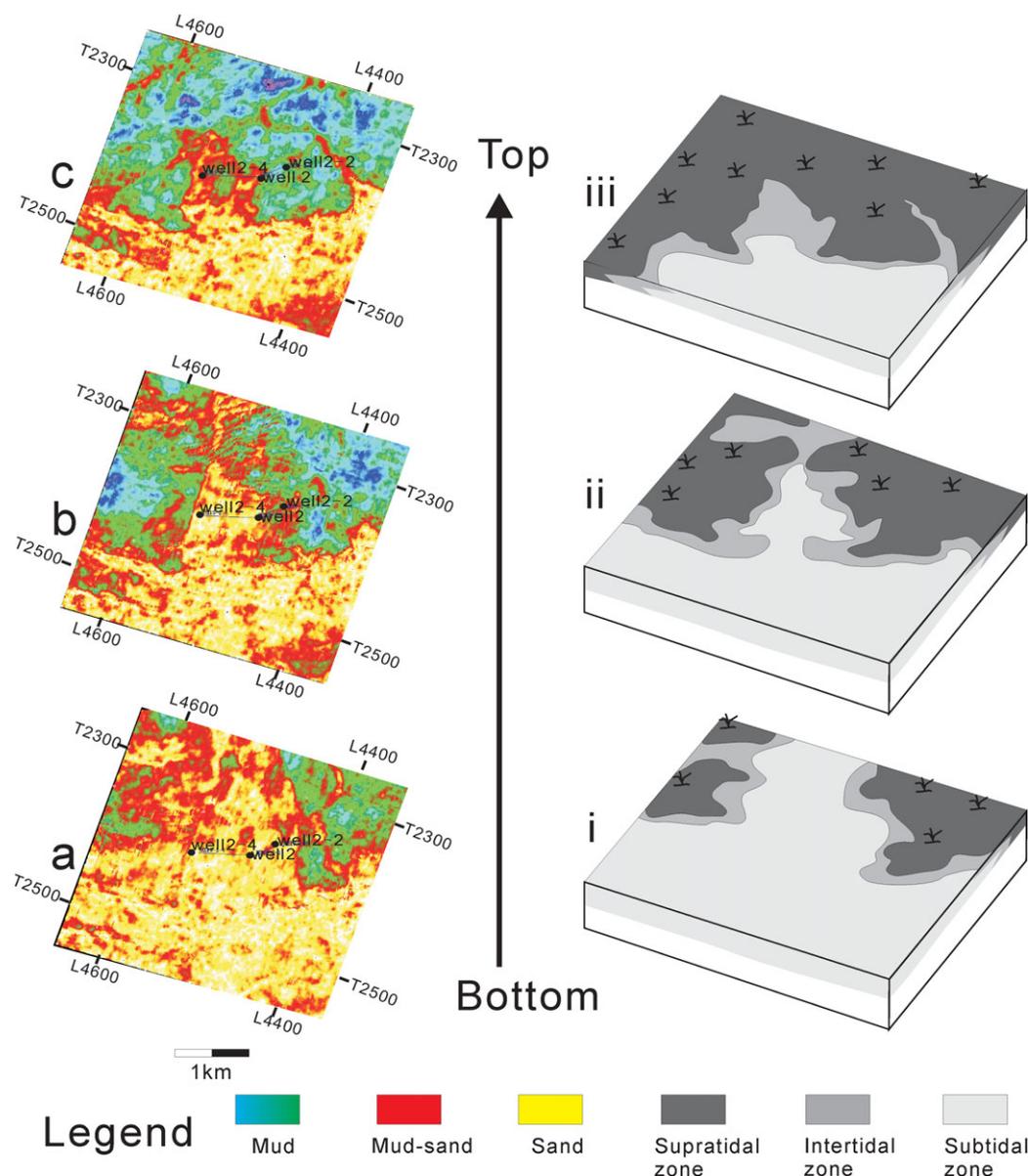
Figure 10. Attribute maps of RMS amplitude extracted from stratal slicing and evolution of tidal deposition in Cycle 5. The tidal mud flat progrades seawards gradually, which displays as tidal deposition stepping seawards in response to base level fall.

with all the available geological information. In the calibration of the well logging and the RMS amplitude, yellow (low RMS amplitude) means a high sand ratio subtidal zone, red (medium RMS amplitude) means a medium sand/mud ratio intertidal zone, while green and blue (high RMS amplitude) means a high mud ratio supratidal zone.

The funnel shape of an estuary tends to increase the flood-tidal current strength, but it decreases the landward extent of tidal effects in an estuary to zero at the tidal limit. The yellow zone occupies most of the study area in the lower part of Cycle 5 (Fig. 10a). The blue and green zone expands and occupies half of the study area in the middle of Cycle 5 (Fig. 10b). The blue and green zone cut by red belts greatly enlarges and dominates the main part of the study area in the upper part of Cycle 5 (Fig. 10c). The blue and green zone shows the scope of the supratidal zone, and the

yellow zone designates sandy sedimentation consisting of a tidal channel, bar and sand flat deposits (Fig. 10a, b, c).

The northern part of the study area is mainly a supratidal mud flat, and the southern part is dominated by subtidal sand deposits. From the bottom to the top of Cycle 5, the mud flat progrades seawards and behaves like a tidal estuary stepping seawards in response to the base level fall (Fig. 10i, ii, iii). The clear boundary between the green and yellow zone helps map the distribution and geometry of the reservoir.

6. Discussion

The major reservoir of the tidal succession is composed of tidal channel, creek, bar and sand flat sandstones of subtidal and intertidal zones. The scale and thickness of the tidal sandstone increases seawards along plane

(Fig. 10). The progradation of tidal flats in response to a falling base level forms a fining-upwards cycle that, in an assemblage of sandstone at the bottom and coal beds and mud layers at the top, are a favourable reservoir-seal group. Vertically, the intertidal and supratidal zones in the upper parts of the tidal cycle are of high oil saturation (Fig. 8). The intertidal zone or the upper part of a tidal cycle is a favourable area for prospecting and oil reserves.

7. Conclusions

Based on an analysis of the stratigraphy of a tidal succession, we correlated the sequence boundaries of the tidal deposits and built the isochronous framework of Cycle 5 in the Zhuhai Formation. Through stratal slicing, we imaged the distribution of tidal sandstone in a framework of high-resolution sequence stratigraphy. The major conclusions include the following:

(1) The tidal flat progradational allocycle is the result of a long-term base level fall, while the fining-upwards autocycle is in response to a short-term base level fall.

(2) A region-wide mud layer of the supratidal zone and the scour surfaces of the erosive-based tidal channel of the subtidal zone are stratigraphic surfaces of tidal sedimentation.

(3) The tidal sandstone reservoir is located at the coast, and it is displayed as low amplitude on the attribute map of the RMS amplitude extracted from the stratal slicing.

(4) The intertidal zone and the upper part of a tidal cycle are favourable areas for prospecting and oil reserves.

References

BRUCE, S. H. 2002. Validating seismic attribute studies: beyond statistics. *The Leading Edge* **21**, 1016–21.

CARNES, J. B., NOVITSKY-EVANS, J. M., SCHUNK, D. J. & ANONYMOUS. 1994. Structural control on lithofacies in the Zhu 1 Depression, Pearl River mouth basin, South China Sea. *American Association of Petroleum Geologists Bulletin* **78**, 1137.

CHEN, Z. Q., ZHONG, S. L., YANG, S. K. & XU, S. C. 1998. The application of micropalaeontology in sequence stratigraphy; an example from the Huizhou Depression in the South China Sea. *Acta Micropalaeontologica Sinica* **15(2)**, 134–43.

CHOPRA, S. & MARFURT, K. J. 2008. Emerging and future trends in seismic attributes. *The Leading Edge* **27**, 298–318.

CROSS, T. A. 1992. There are no gaps in the stratigraphic record. In *Annual Meeting Expanded Abstracts – American Association of Petroleum Geologists* (**1992**), 24–5.

DENG, H. W. & ZHENG, W. B. 2009. Depositional characteristics of offshore tidal deposits in the Lower Tertiary Zhuhai Formation, Huizhou Depression, Pearl River Mouth Basin. *Geoscience* **23(5)**, 767–75 (in Chinese with English abstract).

EVANS, G. 1975. Intertidal flat deposits of the Wash, western margin of the North Sea. In *Tidal Deposits: A casebook of recent examples and fossil counterparts* (ed. R. N. Ginsburg), pp.13–20. Berlin: Springer-Verlag.

HORN, B. W., CROSS, T. A., HORNBECK, J. A. & ZAVALA, M. 2001. Stratigraphic controls on reservoir strata: a comparison of fluvial and tidal reservoirs in the Almond Formation, Coal Gulch, Wamsutter, Echo Springs, and Table Rock fields, Washakie Basin, Wyoming. In *Wyoming Gas Resources and Technology: Wyoming Geological Association, 52nd Field Conference Guidebook* (ed. D. P. Stilwell), pp. 149–61.

LI, X. Y., ZHENG, R. C., WEI, Q. L., WANG, J. & GEN, W. 2007. Characters of the sedimentary facies of Paleogene Zhujiang Formation in Huizhou Depression, Zhujiangkou Basin, China. *Journal of Chengdu University of Technology* **34(3)**, 251–8.

MACKENZIE, D. B. 1972. Tidal sand flat deposits in Lower Cretaceous Dakota Group near Denver, Colorado. *The Mountain Geologist* **8**, 141–50.

REINECK, H. E. 1972. Tidal flats. In *Recognition of Ancient Sedimentary Environments* (ed. J. K. Rigby), pp.146–59. Society of Economic Paleontologists and Mineralogists, Special Publication no. 16.

SHANMUGAM, G., POFFENBERGER, M. & TORO ALAVA, J. 2000. Tide-dominated estuarine facies in the Hollin and Napo ('T' and 'U') Formations (Cretaceous), Sacha Field, Oriente Basin, Ecuador. *American Association of Petroleum Geologists Bulletin* **84**, 652–82.

SHANLEY, K. W. & MCCABE, P. J. 1991. Predicting facies architecture through sequence stratigraphy – an example from the Kaiparowits Plateau, Utah. *Geology* **19**, 742–5.

VAN WAGONER, J. C. 1990. Sequence boundaries in siliciclastic strata on the shelf; physical expression and recognition criteria. In *Abstracts, Distinguished Lecture Tours, 1990–1991. American Association of Petroleum Geologists Bulletin* **74**, 1774–5.

WEI, Q. L., ZHENG, R. C., SHI, H. S., DU, J. Y. & LI, X. Y. 2008. High resolution sequence stratigraphic characteristics of the Paleogene Zhuhai Formation in Huizhou depression marine delta. *Acta Sedimentologica Sinica* **26(5)**, 744–52.

WHEELER, H. E. 1964. Base level, lithosphere surface, and time-stratigraphy. *Geological Society of America Bulletin* **75**, 599–610.

ZENG, H. L., BACKUS, M. M., BARROW, K. T. & TYLER, N. 1998. Stratal slicing: Part I, realistic 3-D seismic model. *Geophysics* **63**, 502–13.